2011

Detection of cardiac myosin heavy chain-α-specific CD4 cells by using MHC class II/IA^k tetramers in A/J mice

Chandirasegara Massilamany
University of Nebraska-Lincoln, cmassilamany@unl.edu

Arunakumar Gangaplara
University of Nebraska-Lincoln

Nora M. Chapman
University of Nebraska Medical Center, nchapman@unmc.edu

Noel Rose
Johns Hopkins School of Medicine, nrrose@jhsph.edu

Jay Reddy
University of Nebraska - Lincoln, jayreddy@unl.edu

Published in *Journal of Immunological Methods* 372:1–2 (2011), pp. 107–118
doi: 10.1016/j.jim.2011.07.004

Submitted October 28, 2010; revised June 13, 2011; accepted July 5, 2011;
published online July 18, 2011.

Detection of cardiac myosin heavy chain-α-specific CD4 cells by using MHC class II/IA^k tetramers in A/J mice

Chandirasegaran Massilamany,[1] Arunakumar Gangaplara,[1] Nora Chapman,[2] Noel Rose,[3] and Jay Reddy [1]

1. School of Veterinary Medicine and Biomedical Sciences, University of Nebraska-Lincoln, Lincoln, NE
2. Department of Pathology and Microbiology, University of Nebraska Medical Center, Omaha, NE
3. Department of Pathology, Johns Hopkins School of Medicine, Baltimore, MD

Corresponding author — J. Reddy, Room 202, Bldg VBS, School of Veterinary Medicine and Biomedical Sciences, University of Nebraska-Lincoln, Lincoln, NE 68583; tel 402 472-8541, fax 402 472-9690, email nreddy2@unl.edu

C. Massilamany and A. Gangaplara were equal contributors and should be considered co-first authors.

Abstract

A/J mice bearing the H-2 allele IA^k are highly susceptible to autoimmune myocarditis induced with cardiac myosin heavy chain (Myhc)-α 334–352, whereas B10.A mice carrying a similar allele IA^k are relatively resistant, suggesting that the generation of Myhc-α-reactive T cell repertoires is influenced by genetic background. To enumerate the precursor frequencies of Myhc-α-specific CD4 T cells, we sought to create IA^k tetramers for Myhc-α 334–352. Tetramers were created using approaches that involve covalent tethering of individual peptide sequences or exogenous loading of peptides into empty IA^k molecules by peptide-exchange reaction. Using ribonuclease 43–56 tetramers as controls, we demonstrated that by flow cytometry (FC), Myhc-α 334–352 tetramers specifically bind myosin-reactive T cells. CD4 cells isolated from A/J mice immunized with Myhc-α 334–352 were used to optimize conditions for tetramer staining, and neuraminidase treatment prior to tetramer staining permitted the detection of Myhc-α-specific cells *ex vivo*. The reagents are useful tools for monitoring the frequency of Myhc-α-reactive CD4 cells and to determine their pathogenic potential at a single cell level by FC.

Keywords: Cardiac myosin, MHC class II tetramers, Myocarditis, Autoimmunity, Mouse model

Abbreviations: DELFIA, dissociation-enhanced lanthanide fluoroimmunoassay; EAM, experimental autoimmune myocarditis; FC, flow cytometry; LN, lymph nodes; LNC, lymph node cells; Myhc-α, cardiac myosin heavy chain-α; NASE, neuraminidase; OE-PCR, overlapping extension polymerase chain reaction; Tet, tetramer

1. Introduction

Several animal models of experimental autoimmune myocarditis (EAM) have been developed in various rodent species to study the immunological mechanisms of myocardial injuries. Autoimmune myocarditis can be induced in susceptible animals by immunizing the animals with myocarditogenic epitopes of cardiac myosin heavy chain (Myhc)-α; the disease is mediated primarily by CD4 T cells (Liao et al., 1993; Donermeyer et al., 1995). The disease-inducing epitopes of Myhc-α have been characterized in mice and rats, notably Myhc-α 334–352 in A/J (H-2^a), CBA/J (H-2^k) and B10.A (H-2^k) mice; Myhc-α 614–643 in BALB/c (H-2^d) mice; and Myhc-α 1304–1320 in Lewis rats (RT1) (Neu et al., 1987b; Kodama et al., 1990; Smith and Allen, 1991; Donermeyer et al., 1995; Pummerer et al., 1996). Myhc has two isoforms, Myhc-α and Myhc-β, which are expressed at different times during development. Myhc-α is expressed in adult mice, whereas Myhc-β is expressed in the fetus (Pummerer et al., 1996; Reiser et al., 2001; Hill et al., 2002), suggesting that the T cell repertoire of the Myhc-α form may have escaped tolerance mechanisms in the thymus. The fact that myocarditis could be induced with only Myhc-α but not Myhc-β raises a question whether susceptible mice

have endogenously derived a Myhc-α-specific T cell repertoire, which expands upon immunization with myosin.

Our studies involve A/J mice carrying the H-2 allele IA^k at the major histocompatibility complex (MHC) class II locus, which are highly susceptible to EAM induced with Myhc-α 334–352 (Donermeyer et al., 1995). In contrast, B10.A mice, which also carry the IA^k allele, are relatively resistant, suggesting that both MHC and non-MHC genes contribute to susceptibility to myocarditis (Neu et al., 1987b). To investigate these genetic differences, we created IA^k tetramers for Myhc-α 334–352. Using bovine ribonuclease (RNase) 43–56 tetramers as controls, we demonstrated that Myhc-α 334–352 tetramers bind myosin-reactive cells with specificity, and the reagents are useful in detecting antigen-specific cells *ex vivo*.

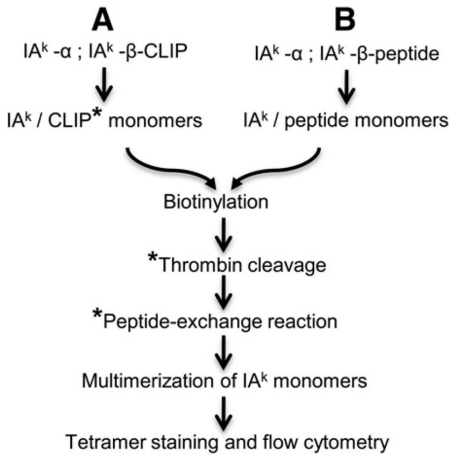

Figure 1. Strategies adopted to create IA^k tetramers. A, derivation of tetramers from CLIP precursors. This approach involved covalent tethering of the nt sequence of CLIP 88–102 into the IA^k-β construct, followed by expression of soluble IA^k molecules, biotinylation, thrombin cleavage, peptide loading and tetramerization. B, derivation of tetramers from peptide precursors. In this approach, the nt sequences of Myhc-α 334–352 and RNase 43–56 were covalently tethered into the IA^k-β construct such that IA^k monomers containing the peptides were expressed directly. *Steps pertaining to CLIP precursors only.

2. Materials and methods

2.1. Mice

We used 6- to 8-week-old female A/J mice ($H\text{-}2^a$), obtained from the Jackson Laboratory (Bar Harbor, ME) and maintained in accordance with the guidelines of the University of Nebraska-Lincoln.

2.2. Peptide synthesis and immunization procedures

Myhc-α 334–352 (DSAFDVLSFTAEEKAGVYK), and RNase (VNTFVHESLADVQA) were synthesized on 9-fluorenylmethyloxycarbonyl chemistry (Neopeptide, Cambridge, MA). All peptides were HPLC-purified (> 90%), identity was confirmed by mass spectroscopy, and the peptides were dissolved in 1× PBS prior to use. For immunizations, peptides were emulsified in complete Freund's adjuvant (CFA) supplemented with *Mycobacterium tuberculosis* extract to a final concentration of 5 mg/ml, and administered subcutaneously in multiple sites in the flank, footpads and sternal regions (100 μg/mouse) (Donermeyer et al., 1995; Pummerer et al., 1996).

2.3. Creation of IA^k constructs and expression of soluble IA^k monomers

Full length cDNAs representing IA^k-α and IA^k-β chains were synthesized by RT-PCR using total RNA extracted from splenocytes stimulated with lipopolysaccharide and interferon-γ. To express soluble IA^k molecules, transmembrane and cytoplasmic regions of IA^k-α and IA^k-β chains were replaced with the leucine zipper domains of Fos and Jun transcriptional factors, respectively, as described previously (Jang et al., 2003; Reddy et al., 2003). We adopted two approaches to create IA^k tetramers (Figure 1).

2.3.1. Derivation of tetramers using MHC class II-associated invariant chain peptide (CLIP) precursors

This approach involved covalent tethering of nt sequences of CLIP 88–102 (gtgagccagatgcggatggctactcccttgctgatgcgtccaatg) into the IA^k-β construct such that upon expression, CLIP-linked IA^k proteins were obtained and tetramers could then be derived by exchanging CLIP with peptides of interest (Day et al., 2003; Jang et al., 2003).

IA^k-α construct. First, we amplified the sequence of extracellular (E/C) domain from full length IA^k-α cDNA, including the leader sequence, and the fragment was flanked by *Bam H I* (5′) and *Sal I* (3′) sites. Second, a fragment containing Fos and the BiR-A site for biotinylation was synthesized by overlapping extension PCR (OE-PCR) to include *Sal I* and *Bam H I* sites at 5′ and 3′ ends, respectively. The two fragments were then ligated using *Sal I* and cloned into the *Bam H I* site in p10 dual promoter-containing pAcDB3 vector (BD Pharmingen, San Diego, CA). The final IA^k-α construct should then have contained, in the order of leader sequence: E/C domain, linker (GGGGG), Fos (LTDTLQAETDQLEDEKSALQTEIANLLKEKEKLEFILAA), linker (SAGGG) and BiR-A site (GLNDIFEAQKIEWHE).

IA^k-β construct. Generation of the IA^k-β construct required three cassettes. Cassette 1: PCR product was synthesized by OE-PCR to include leader sequence, *Kpn I* site, CLIP 88–102 (VSQMRMATPLLMRPM), linker (GGGGS), thrombin cleavage site (LVPRGS), and *Bam H I*/linker (GSGSGS). Cassette 2: PCR product flanked by *Bam H I* (5′) and *Sal I* (3′) sites, generated from full-length IA^k-β cDNA to include E/C region of IA^k-β, was obtained. Cassette 3: PCR product flanked by *Sal I* (5′) and *EcoR I* (3′) sites representing the Jun sequence was amplified from IA^s/myelin proteolipid protein (PLP) 139–151 construct (a kind gift from Dr. Vijay Kuchroo, Harvard University, Boston, MA) (Reddy et al., 2003). We ligated cassettes 2 and 3 first, followed by cassette 1, and the full-length construct thus derived was cloned into *Bgl II* and *EcoR I* sites in pAcDB3 vector and sequenced.

2.3.2. Derivation of tetramers using peptide-precursors

In this approach, nt sequences of Myhc-α 334–352 and RNase 43–56 were tethered into the IA^k-β construct, which permitted

expression of peptide-linked monomers directly (Massilamany et al., 2010). We used the IA^k-α construct designed to obtain CLIP precursors and modified the IA^k-β construct by replacing the sequences of CLIP and thrombin cleavage site with Myhc-α334–352 (gatagtgcctttgatgtgctgagcttcacggcagaggagaaggctggtgtctacaag) or RNase 43–56 (gtgaacacctttgtgcacgagtccctggctgatgtccaggcc).

The soluble IA^k molecules were expressed in a Baculovirus system using sf9 insect cells as described previously (Reddy et al., 2003; Massilamany et al., 2010). Briefly, large-scale protein production was performed in suspension cultures grown in spinner flasks attached to a sparger system (Bellco, Vineland, NJ) at a multiplicity of infection 5. Cells were grown at a density of 1×10^6 cells/ml in protein-free insect cell medium (SF900 III SFM, Invitrogen, Carlsbad, CA) for 3 to 5 days; the supernatants were concentrated using a Prep/Scale-TFF cartridge (30 kDa) (Millipore, Bellerica, MA) and purified on anti-IA^k column (clone, 10–2.16). The protein elutes were concentrated using Amicon ultra centrifugal filters (Millipore), and the protein yield typically ranged from 1 to 1.6 mg/l, regardless of IA^k constructs used.

2.4. Biotinylation, thrombin cleavage, peptide-exchange and tetramerization

Biotinylation of IA^k proteins was performed using biotin protein ligase (Avidity, Denver, CO) at 30 °C in a reaction mixture containing 25 μg/10 nM of enzyme and 2.5 mg/ml of IA^k proteins (Reddy et al., 2003). After overnight incubation, free biotin was removed by dialysis using ice-cold 1× PBS in multiple cycles over a period of 24 h.

Thrombin digestion was carried out at room temperature (RT) for 2 h in 10 mM Tris HCl, pH 8.0, consisting of biotinylated IA^k proteins (1–2 mg/ml) and thrombin (20 units/mg) (Novagen, Madison, WI; Day et al., 2003; Jang et al., 2003). Thrombin-cleaved IA^k proteins were resolved in 12% sodium dodecyl sulfate (SDS)-polyacrylamide gel electrophoresis (PAGE) analysis and the migration pattern of the IA^k-β chain was compared with uncleaved IA^k protein.

To validate conditions for peptide-exchange reactions, we used dinitrophenol (DNP)-labeled Myhc-α 334–352 or RNase 43–56 in which a DNP tag was attached with one aminohexanoic acid linker at the N-terminus. The peptide purity (> 92%) was verified by mass spectrometry and HPLC (Neopeptide; Day et al., 2003; Jang et al., 2003). The conditions used for optimization included temperature, concentration of IA^k proteins and peptides (molar ratios, 3.3 μM:16.5 μM to 3.3 μM:132 μM) and pH (5.5 to 7.5). Briefly, thrombin-cleaved, unbiotinylated IA^k monomers and DNP-Myhc-α 334–352 were incubated in duplicates in a peptide-exchange buffer containing sodium phosphate 50 mM, sodium chloride 100 mM, EDTA 1 mM and 1× protease inhibitor overnight at RT. The reaction mixture was coated onto 96-well white fluorescence plates (Nunc, Rochester, NY) in sodium phosphate 0.2 M, pH 6.8 overnight at 4 °C. The plates were washed 5 times with 1× wash buffer (Perkin Elmer, Waltham, MA) and blocked with casein 2% for 2 h at 37 °C. After washing as above, biotinylated anti-DNP was added (0.25 μg) to each well (American Research Products, Belmont, MA) and incubated for 1 h at RT. Europium-labeled streptavidin (SA) was then added to a concentration of 1 μg/ml of dissociation-enhanced lanthanide fluoroimmunoassay (DELFIA) buffer followed by DELFIA-enhancement solution (Perkin Elmer; Jang et al., 2003). Fluorescence intensity was measured at excitation/emission wavelengths of 340/615 nm using a Victor^3 Multi Label Plate Reader (Perkin Elmer). The optimized conditions were then used to generate tetramers utilizing biotinylated thrombin-cleaved IA^k proteins and unlabeled Myhc-α 334–352 or RNase 43–56.

2.5. Western blotting analysis

IA^k-α and IA^k-β chains contained the leucine zipper domains of Fos and Jun, respectively (Reddy et al., 2003). The soluble IA^k molecules in the Baculovirus-infected supernatants were resolved in 12% SDS-PAGE analysis and probed with rabbit anti-Fos and anti-Jun polyclonal sera (a kind gift from Dr. Vijay Kuchroo) (Reddy et al., 2003). The Fos- and Jun-antibody complexes were captured by goat anti-rabbit secondary antibody conjugated with horseradish peroxidase, and the signals were detected by enhanced chemiluminescence (ECL).

2.6. Measurement of recall responses

Ten days after immunization with Myhc-α 334–352 or RNase 43–56, mice were killed and the draining lymph nodes (LN) (maxillary, mandibular, popliteal, axillary and inguinal) were harvested. Single cell suspensions were prepared after lysing the erythrocytes with 1× ammonium chloride potassium buffer (Lonza, Walkersville, MD). Lymph node cells (LNC) were stimulated with the indicated peptides (0–100 μg/ml) at a cell density of 5×10^6 cells/ml for 2 days in growth medium containing 1× RPMI supplemented with 10% fetal calf serum (FCS), 1 mM sodium pyruvate, 4 mM l-glutamine, 1× each of non-essential amino acids and vitamin mixture, and 100 U/ml penicillin–streptomycin (Lonza). Cultures were then pulsed with 1 μCi of tritiated ^{3}[H] thymidine per well; 16 h later, proliferative responses were measured as counts per minute (cpm) using the Wallac liquid scintillation counter (Perkin Elmer; Reddy et al., 2003; Massilamany et al., 2010).

2.7. IA^k tetramer staining

IA^k/Myhc-α 334–352 and RNase 43–56 tetramer staining was performed by three- or four-color flow cytometry (FC) as we have previously described (Massilamany et al., 2010). LNC obtained from mice immunized with Myhc-α 334–352 or RNase 43–56 were restimulated with the corresponding peptides (50 μg/ml), and after 2 days growth medium containing interleukin (IL)-2 was supplemented. Viable lymphoblasts were harvested on day 5 poststimulation by Ficoll-density gradient centrifugation and the cells were maintained in IL-2 medium. Tetramer staining was performed by incubating the cells with IA^k/Myhc-α 334–352 or RNase 43–56 tetramers conjugated with phycoerythrin (PE) in growth medium, pH 7 to 8.2, at 4 °C, 37 °C or RT for 0.5 to 3 h. Cells were washed twice with 5 ml of 1× PBS and incubated with anti-CD4, anti-CD25 or anti-CD40 ligand (CD40L) (eBioscience, San Diego, CA), and 7-aminoactinomycin D (7-AAD; Invitrogen) on ice for 20 min. After washing as above, cells were acquired by a

flow cytometer (FACScan or FACSCalibur, BD Biosciences, San Diego, CA), and the frequency of tetramer (tet)$^+$ cells was then enumerated by using Flow Jo software (Tree Star, Ashland, OR) in the live (7-AAD$^-$) population. Tetramer staining was optimized with respect to concentration of tetramers, duration, temperature, pH and the amount of FCS in the staining medium. The reaction conditions for each of the parameters were as follows: concentration of tetramers, and temperature (RT for 3 h, FCS 2.5%, pH 7.6); duration (RT, FCS 2.5%, pH 7.6); pH (RT for 3 h, FCS 2.5%) and amount of FCS (RT for 3 h, pH 7.6).

2.8. Effect of neuraminidase (NASE) on IA^k/tetramer staining

Myhc-α 334–352 reactive cell cultures were prepared from A/J mice as above and the cells were maintained in IL-2 medium for 2 weeks. Cells were then treated with or without NASE (0.7 units/ml) (Type X from *Clostridium perfringens*, Sigma-Aldrich, St. Louis, MO) in serum-free 1× DMEM for 45 min at 37 °C at a density of 1×10^7 cells/ml (Reddy et al., 2003). After washing once with 5 ml of 1× PBS, cells were stained with tetramers, anti-CD4 and 7-AAD and acquired by FC. Tet$^+$ cells were analyzed in the live (7-AAD$^-$) CD4 subset.

2.9. Detection of Myhc-α 334–352-reactive CD4 cells by IA^k tetramer staining ex vivo

A/J mice were immunized with Myhc-α 334–352 in CFA twice with an interval of 1 week. After 7 days, the mice were killed and LNC were prepared and used to determine the effect of NASE on T cells. LNC were treated with or without NASE as above followed by staining with CD4, CD69, CD25, CD44 and CD62 ligand (CD62L) antibodies and 7-AAD. After acquiring the cells by FC, percentages of each marker were determined in the live (7-AAD$^-$) CD4 subset. For tetramer analysis, LNC were obtained from a pool of draining LN obtained from three to five mice in each experiment. CD4 cells were enriched to a purity of more than 95% by negative selection based on magnetic separation using IMAG according to the manufacturer's recommendations (BD Biosciences). After treating the cells with or without NASE as above, cells were incubated with tetramers (30 μg/ml) for 3 h at RT in growth medium, pH 7.6, supplemented with FCS (2.5%). Cells were washed twice with 5 ml of 1× PBS and stained with anti-CD4, anti-CD25, and 7-AAD and acquired by a flow cytometer (FACSCalibur, BD Biosciences). The live (7-AAD$^-$) CD25$^+$ cells were gated first in relation to forward scatter (FSC) and in which tet$^+$ cells were determined corresponding to CD4 subset.

2.9.1. Enrichment of tet$^+$ cells by magnetic separation

Tetramer-positive cells were enriched using anti-PE magnetic particles as described previously (Day et al., 2003; Jang et al., 2003). Briefly, A/J mice were immunized with Myhc-α 334–352 in CFA twice with an interval of 1 week. Seven days after the second immunization, draining LN were pooled from groups of three to five mice each and LNC were obtained. CD4 cells were enriched to a purity of more than 95% (as described in Section 2.9) and stained with PE-conjugated IA^k tetramers (30 μg/ml) for 3 h at RT in growth medium containing 2.5% FCS, pH 7.6. Cells were washed with 1× BD IMag buffer and incubated with anti-PE magnetic particles for 30 min at 4 °C. The anti-PE-bound tet-PE$^+$ cells were then enriched using IMag as recommended (BD Biosciences). Cells were stained with anti-CD4 and 7-AAD and acquired by a flow cytometer (FACSCalibur, BD Biosciences) and the percentages of tet$^+$CD4$^+$ cells were then enumerated in the live (7-AAD$^-$) subset using Flow Jo software. To enrich tet$^+$ cells from *in vitro* expanded cultures, viable lymphoblasts harvested on day 8 poststimulation with Myhc-α 334–352 were used for magnetic separation as described above.

3. Results

3.1. Creation of IA^k tetramers

IA^k tetramers were created utilizing CLIP or peptide precursors (Figure 1). The IA^k constructs corresponding to each approach were designed and successfully expressed in a Baculovirus system (Figure 2). We confirmed the identity of IA^k-α and IA^k-β chains by Western blotting analysis by testing anti-Fos

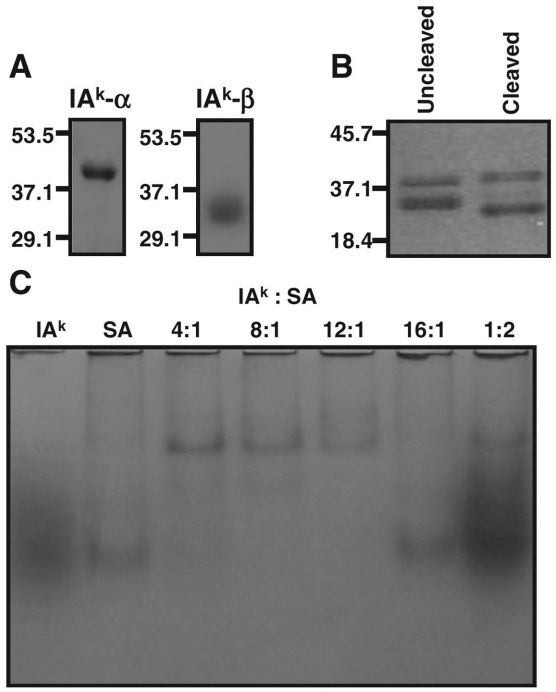

Figure 2. Derivation of IA^k tetramers. A, IA^k protein expression. IA^k constructs representing the extracellular domains of IA^k-α and IA^k-β chains were designed to include Fos and Jun sequences, respectively, and the soluble IA^k proteins were expressed in Baculovirus using sf9 insect cells. After purifying the monomers on an anti-IA^k column (10-2.16), the identity of IA^k-α and IA^k-β chains was verified by Western blotting analysis using rabbit anti-Fos and anti-Jun polyclonal sera and peroxidase-conjugated anti-rabbit secondary antibody, and the signals were detected by ECL. B, thrombin cleavage. Biotinylated IA^k monomers containing CLIP 88–102 were digested with thrombin to release CLIP, and the proteins were resolved in 12% SDS-PAGE analysis and stained with Coomassie blue. C, multimerization of IA^k monomers. IA^k proteins were biotinylated using biotin protein ligase, and the free biotin molecules were removed by dialysis in 1× PBS. Biotinylation was verified by mixing biotinylated proteins and SA at the indicated molar ratios and the multimerized complexes were resolved in 6% native PAGE analysis. Representative data from three individual experiments are shown.

and anti-Jun polyclonal rabbit sera, and protein bands of expected sizes (IA^k-α, ~ 40 kDa; IA^k-β, ~ 30 kDa) were obtained (Figure 2A). The CLIP-linked strategy required thrombin cleavage to facilitate the release of the CLIP from the IA^k-β chain. Thrombin at a concentration of 20 units/mg for 2 h at RT led to complete cleavage as indicated by greater migration of IA^k-β chain, compared with the uncleaved protein (Figure 2B). For initial validation, we sought to create tetramers utilizing peptide precursors, which involved biotinylation and multimerization of IA^k monomers using fluorescent dye-labeled SA. The extent of biotinylation was confirmed by mixing biotinylated IA^k proteins with SA; the molar ratios of 4:1 to 8:1 resulted in the formation of comparable amounts of higher molecular weight complexes (Figure 2C). We chose a molar ratio of 4:1 to prepare tetramers for flow cytometric evaluation of antigen-specific cells using SA-PE.

3.2. IA^k tetramers bind antigen-sensitized T cells with specificity

To determine the specificity of IA^k tetramers, we used primary T cell cultures obtained from A/J mice immunized with Myhc-α 334–352 or RNase 43–56. We verified that the animals responded to the antigens based on tritiated ^{3}[H] thymidine incorporation assay. Although RNase 43–56 was less immunogenic than Myhc-α 334–352, both peptides induced dose-dependent T cell responses (Figure 3A). For tetramer staining, LNC were first stimulated with peptides and cultured in IL-2 contained medium. After 5 days, viable cells were harvested and stained with Myhc-α 334–352 or RNase 43–56 tetramers, such that one of the two tetramers served as control in its respective antigen-sensitized cultures; the tet^+ cells were enumerated by FC. Myhc-α tetramers bound cells obtained from mice immunized with Myhc-α 334–352 (1.95%), but not from those immunized with RNase 43–56 (0.07%); the converse also was true of RNase 43–56 tetramers (RNase 43–56—0.63% and Myhc-α 334-352—0.08%; Figure 3B). The lower frequency of RNase tet^+ cells is possibly due to the relatively poor response obtained in the immunized mice. To further verify the specificity of IA^k tetramers, we adopted a strategy of enriching tet^+ cells using anti-PE magnetic particles (Day et al., 2003; Jang et al., 2003). Expectedly, Myhc-α 334–352 tet^+ cells were enriched antigen-specifically as indicated by an increase in the number of Myhc-α 334–352 tet^+ cells in the post-enriched fraction (4.01%) as opposed to 0.61% in the pre-enriched fraction with a difference of ~ 6.6 fold between the two (Figure 3C). Such an increment was negligible with RNase 43–56 tetramers. Taken together, the results suggest that IA^k tetramers specifically bind antigen-sensitized CD4 cells.

3.3. Optimized conditions for IA^k tetramer staining

For routine applications of tetramers, it was critical to optimize conditions, and our goal was to enhance tetramer binding without compromising specificity. We considered the parameters of concentration, duration, temperature, pH and the composition of the tetramer staining medium in experiments involving Myhc-α 334–352-reactive cells (Figure 4). We noted that the intensity of tetramer staining was enhanced in proportion to the increased concentration of tetramers (10–60 μg/ml). Such an enhancement was also evident when the duration for tetramer

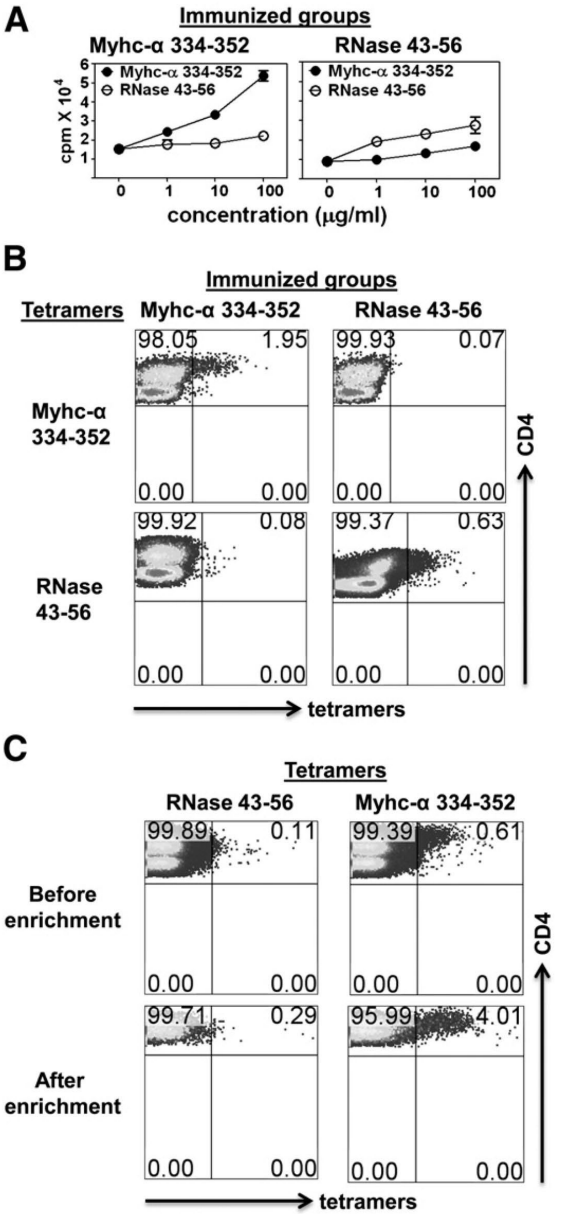

Figure 3. Specificity of IA^k/tetramer staining. A, proliferation response. A/J mice were immunized with Myhc-α 334–352 or RNase 43–56 in CFA. After 10 days, the mice were killed and LN from three to four mice were pooled and single cell suspensions were prepared. LNC were stimulated with the corresponding peptides for 2 days and, after pulsing with tritiated ^{3}[H] thymidine during the last 16 h, proliferative responses were measured as cpm. Mean ± SEM values from three individual experiments involving 3 to 4 mice in each are shown. B, specificity of IA^k tetramers. LNC obtained from immunized mice with Myhc-α 334–352 or RNase 43–56 (control) were restimulated as above and the cells were maintained in IL-2 medium. Viable lymphoblasts were harvested on day 9 and stained with IA^k/tetramers and anti-CD4 and 7-AAD. After acquiring the cells by FC, tet^+ cells were analyzed in the live ($7\text{-}AAD^-$) CD4 subset. Representative data from three to five individual experiments each involving 3 to 4 mice are shown. C, enrichment of tet^+ cells by magnetic separation. Lymphoblasts were harvested from cultures stimulated with Myhc-α 334–352 on day 8 poststimulation and stained with PE-conjugated Myhc-α 334–352 or RNase 43–56 tetramers followed by anti-PE magnetic particles and the anti-PE-bound fractions were enriched based on magnetic separation. The enriched fractions were then washed and stained with anti-CD4 and 7-AAD and after acquiring the cells by FC, anti-PE-bound tet^+ cells were analyzed. Data shown represent two individual experiments each involving 3 to 4 mice.

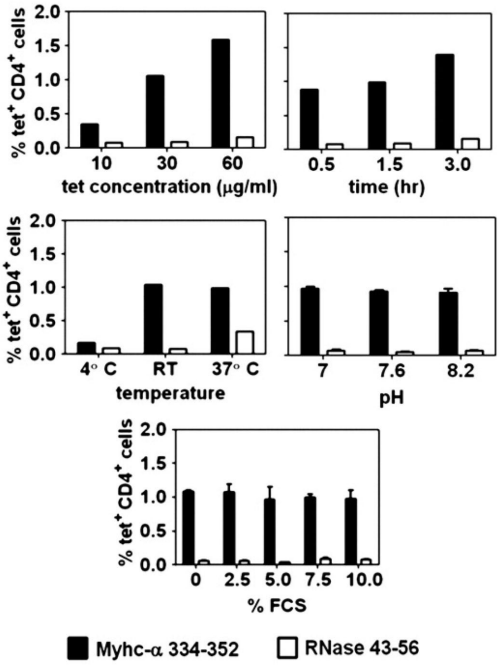

Figure 4. Optimization of reaction conditions for IA^k tetramer staining. Myhc-α 334–352-reactive T cells were used to optimize conditions for IA^k tetramer staining by FC involving tetramers, anti-CD4 and 7-AAD. The reaction conditions were concentration of tetramers, duration of tetramer staining, temperature of staining reactions, pH and concentration of FCS in the staining medium. Shown are the percentages of tet^+ cells in the live ($7\text{-}AAD^-$) CD4 subset. RNase 43–56, control. Representative data from two individual experiments are shown.

binding was prolonged (0.5–3 h). Temperature had a significant effect on tetramer binding: staining was negligible at 4 °C when compared with 37 °C or RT. Although the intensity of tetramer staining was comparable at both RT and 37 °C (~ 1%), the background staining for RNase 43–56 tetramers was least at RT. Equivalent intensity of tetramer staining (~ 1%) was obtained regardless of either pH (7 to 8.2) or the amount of FCS present in the tetramer staining medium. Based on these results, we chose a concentration of 30 μg/ml of tetramers, 3 h duration, RT, a medium containing 2.5% FCS and IL-2 (5 μM), and pH 7.6 as the ideal conditions for tetramer staining.

3.4. Myhc-α 334–352 tetramers preferentially stain unactivated or rested cells

We and others have previously shown that MHC class II tetramers have a tendency to bind activated cells, and we sought to verify whether IA^k tetramers also share this feature (Cameron et al., 2001; Novak et al., 2001b; Reddy et al., 2003; Reijonen et al., 2003). Figure 5A shows that Myhc-reactive cells expanded progressively starting on day 4 poststimulation with Myhc-α 334–352. In a similar analysis, Myhc-α 334–352 tetramers failed to bind Myhc-α-reactive cells, nor was significant proliferation in splenocytes obtained from immunized mice (data not shown). We then enumerated the frequency of Myhc-α tet^+ cells in relation to the activation status of antigen-sensitized cells. CD4 expression was upregulated in Myhc-α 334–352-reactive cells as indicated by the appearance of a $CD4^{high}$ population; in addition,

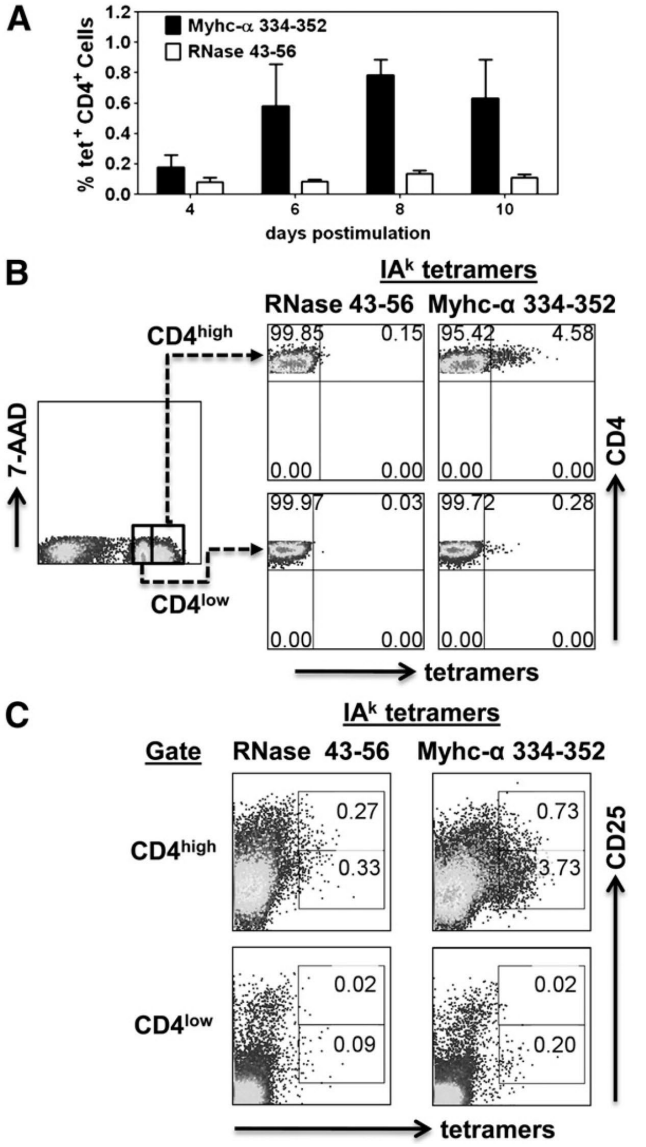

Figure 5. IA^k/Myhc-α 334–352 tetramers preferentially stain activated cells. A, time-course expansion of Myhc-α-reactive cells. LNC from immunized mice were restimulated with Myhc-α 334–352 for 2 days and maintained in IL-2 medium. Viable lymphoblasts were harvested on indicated days and stained with tetramers, anti-CD4 or anti-CD25, and 7-AAD. Cells were acquired by FC, and the percentages of live ($7\text{-}AAD^-$) tet^+CD4^+ cells were then determined. Tetramer analysis was also performed in relation to $CD4^{low}$ *vs.* $CD4^{high}$ (B), or $CD25^{low}$ *vs.* $CD25^{high}$ subsets gated on CD4 cells (C). RNase 43–56, control. Representative data from two to five individual experiments with 3 to 4 mice in each are shown.

Myhc-α 334–352 tetramers preferentially stained $CD4^{high}$ but not $CD4^{low}$ cells (4.58% *vs.* 0.28%; Figure 5B). We next verified tetramer binding in relation to CD25 expression and this was determined by gating $CD4^{high}$ and $CD4^{low}$ subsets. As shown in Figure 5C, Myhc-α 334–352 tetramers bound preferentially to cells expressing $CD25^{low}$ (3.73%) as opposed to $CD25^{high}$ cells (0.73%) within the $CD4^{high}$ subset and such a staining intensity was low in $CD4^{low}$ subset (Figure 5C). The staining of Myhc-α 334–352 tetramers was specific since there was negligible binding to RNase 43–56 tetramers. The facts that CD25 is considered as an activation marker of T cells and that Myhc-α

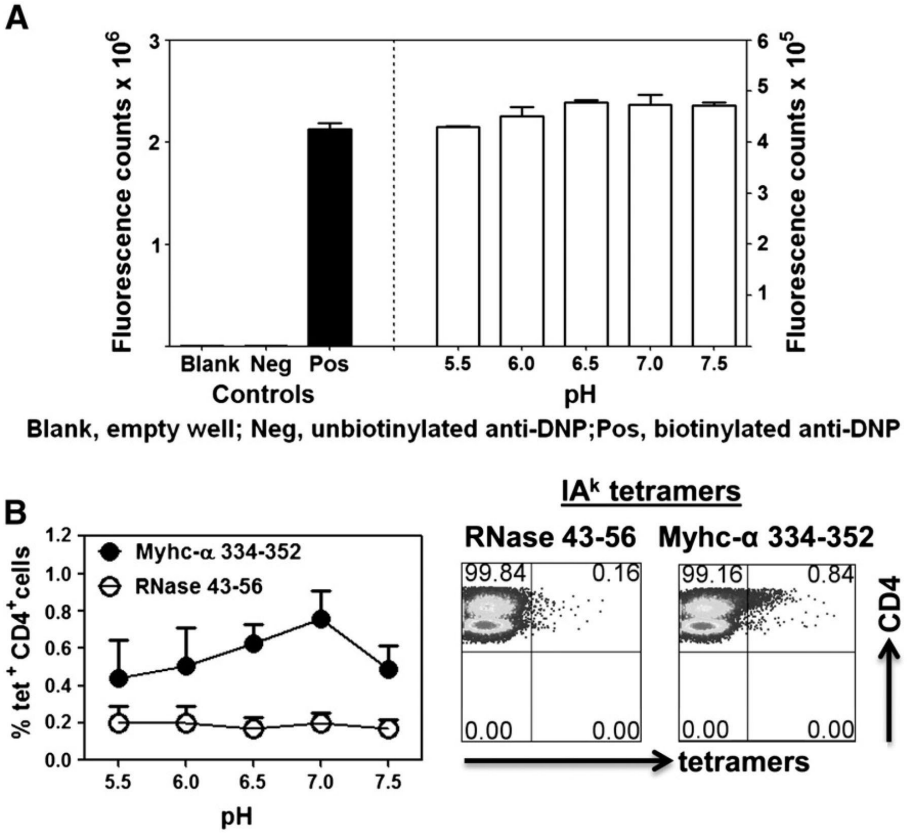

Figure 6. Specificity of IA^k/Myhc-α 334–352 tetramers created based on peptide-exchange reaction. A, peptide-exchange reaction. The CLIP-cleaved IA^k monomers were loaded with Myhc-α 334–352 at 3.3 μM:66.6 μM ratio in peptide-exchange buffer, pH 5.5 to 7.5, overnight at RT. After blocking, biotinylated anti-DNP was added followed by europium-labeled SA in DELFIA buffer and DELFIA-enhancer, and fluorescence counts were measured. Mean ± SEM values representing two individual experiments are shown. B, tetramer staining. The CLIP-cleaved biotinylated IA^k monomers were loaded with Myhc-α 334–352 or RNase 43–56 as above. Tetrameric complexes were then obtained by mixing peptide-loaded IA^k monomers with PE-conjugated SA at 4:1 molar ratio and used to stain Myhc-α-reactive cells by FC. Percentages of tet^+ cells were then enumerated in the live CD4 subset (left panel). Mean ± SEM values are shown (n = 3). The right panel shows the dot plot representation of tetramer staining.

334–352 tetramers bound predominantly to the $CD25^{low}$ but not the $CD25^{high}$ subset suggest that the tetramers have a preference to bind unactivated or rested antigen-specific T cells.

3.5. Validation of IA^k tetramers derived from CLIP-precursors

One of the objectives of deriving tetramers from CLIP-precursors was to be able to create tetramers by loading the peptides of interest exogenously into the CLIP-cleaved empty IA^k molecules (Novak et al., 2001a; Day et al., 2003; Jang et al., 2003). We optimized the conditions for peptide-loading in the IA^k-binding assay, and performed peptide-exchange reactions at different molar ratios (from 3.3 μM:16.5 μM to 3.3 μM:132 μM) and pH (from 5.5 to 7.5) between CLIP-cleaved, IA^k molecules and Myhc-α 334–352. Based on preliminary experiments, 3.3 μM:66.6 μM was an optimal ratio, and, combined with a pH range of 6.0–7.5, resulted in comparable peptide loading (Figure 6A). We then created tetramers by loading Myhc-α 334–352 or RNase 43–56 into biotinylated CLIP-cleaved IA^k molecules followed by multimerization using SA-PE, and the reagents were used to stain Myhc-α 334–352-reactive cells by FC. As shown in Figure 6B, Myhc-α 334–352 tetramers generated under all the pH conditions stained myosin-reactive cells with specificity, but the tetramers prepared at pH 7.0 resulted in maximum staining intensity (0.8%). The data prove that the CLIP precursors could be used to create IA^k tetramers to detect antigen-specific cells.

3.6. Binding of Myhc-α 334–352 tetramers do not correlate with CD40L expression

It has been previously shown that CD40L can be used as a marker of activated antigen-specific cells (Chattopadhyay et al., 2005; Frentsch et al., 2005). We tested whether Myhc-α 334–352 tetramers preferentially bind Myhc-α-specific cells expressing CD40L. We noted that CD40L-expressing cells were evident 3 days after stimulation with Myhc-α 334–352, the expression of which progressively increased, reaching a peak on day 6 followed by a decline (Figure 7A). But the tetramer analysis revealed that only a fraction of these cells bound Myhc-α tetramers (tet^+CD40L^-, 0.67% *vs.* tet^+CD40L^+, 0.13%) (Figure 7B). Similar results were obtained when tetramer analysis was performed in relation to endogenous expression of CD40L based on intracellular staining (data not shown). We also investigated whether blocking CD40–CD40L interaction with CD40 blocking antibody (clone, IC10, eBioscience; Zhang et al., 2007; Baker et al., 2008; Otani et al., 2011) during antigenic stimulation can facilitate stabilization of CD40L such that tet^+ cells can then be

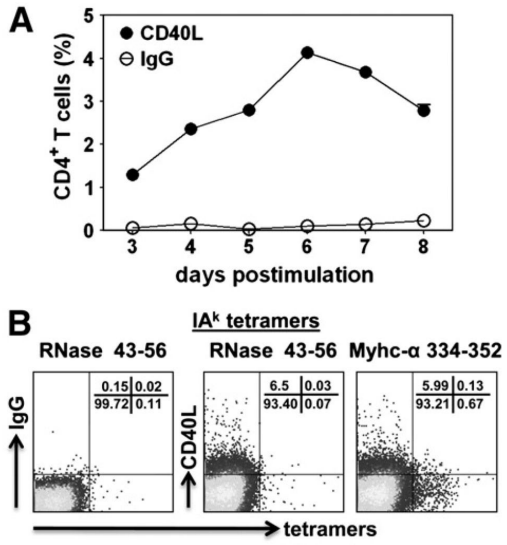

Figure 7. IA^k/Myhc-α 334–352 tetramers stain only a fraction of CD40L-expressing cells. A, time-course expansion of CD40L-expressing CD4 cells. LNC harvested from immunized mice were restimulated with Myhc-α 334–352 for 2 days and rested in IL-2 medium, and CD40L-expressing cells were determined in the live $CD4^+$ subset by FC. B, tetramer analysis. Cells were harvested on day 8 poststimulation, stained with anti-CD40L followed by tetramers, anti-CD4 and 7-AAD and acquired by FC. Percentages of tet^+ cells were then analyzed in relation to CD40L expression within the live (7-AAD^-) CD4 subset. Representative data from three experiments are shown.

better correlated with CD40L-expression. This was not the case as there were no significant differences in the expression levels of CD40L in anti-CD40-treated *vs.* -untreated cells. Likewise, treatment with CD40 blocking antibody did not improve tetramer binding (data not shown). Taken together, our data suggest that binding of Myhc-α 334–352 tetramers does not correlate with CD40L expression in antigen-stimulated cells.

3.7. Enumeration of the frequency of Myhc-α 334–352-reactive cells ex vivo

MHC class II tetramers are useful tools to analyze antigen-specific CD4 cells at a single cell level, but their tendency to stain activated cells limits the use of these reagents *ex vivo*. We previously had shown that the binding ability of IA^s tetramers can be enhanced by treating the cells with NASE prior to tetramer staining, and we adopted this method to detect myosin-specific cells *ex vivo* (Reddy et al., 2003). First, Myhc-α-reactive T cells were generated from immunized mice and the cells were rested for 2 weeks in IL-2 medium. Viable cells were then treated with or without NASE prior to tetramer staining and the tet^+ cells were enumerated by FC. As shown in Figure 8A, NASE treatment enhanced the detection of Myhc-α-specific cells by approximately 4.5 fold (3.2% *vs.* 0.68%). We used these conditions to detect Myhc-α-reactive cells in the LNC obtained from immunized mice *ex vivo*. We noted that NASE activated the cells non-specifically independent of antigen-stimulation as indicated by the appearance of a distinct population composed of large granular cells in which CD69, CD62L, CD44 and, to a lesser degree, CD25 were upregulated (Figure 8B). Corresponding to these markers, we evaluated tetramer staining in cells treated with or without NASE and we found that CD25 was better suited to enumerate antigen-sensitized CD4 cells. Since we could not clearly differentiate $CD25^{low}$ and $CD25^{high}$ subsets, tet^+ cells were enumerated by gating the whole CD25 population. Figure 8C shows that the detection of Myhc-α 334–352 tet^+ cells increased approximately two-fold with NASE treatment (0.28% *vs.* 0.13%). A similar trend was also noted with RNase tetramers, but to a lesser degree (0.07% *vs.* 0.12%), and this level of background staining persisted consistently. Nonetheless, as predicted, the enhanced sensitivity obtained with NASE treatment allowed us to detect more Myhc-α-sensitized cells in immunized mice. Additionally, we also examined Myhc-α 334–352 tet^+ cells in mice that received CFA alone but the reactivity was low (~ 0.07%). To further prove the specificity of Myhc-α 334–352 tetramers, we enriched tet^+ cells corresponding to Myhc-α 334–352 and RNase 43–56 tetramers using anti-PE magnetic particles (Figure 9). Expectedly, the enriched fraction contained 0.92% of Myhc-α 334–352-reactive cells as compared with 0.21% prior to enrichment with a difference of ~ 4 fold and reactivity to RNase 43–56 tetramers was minimal proving that IA^k tetramers can be used to enumerate the frequencies of antigen-specific cells *ex vivo*.

4. Discussion

We have described the generation of IA^k tetramers that allowed us to detect cardiac myosin-specific CD4 cells in mice bearing the H-2 allele, IA^k. Traditionally, limiting dilution analysis and cytokine ELISPOT assay have been used to enumerate the frequencies of antigen-specific cells, but low specificity and the tedious nature of these assays limit their use for routine applications (Buckner et al., 2002; Mallone and Nepom, 2004; Carneiro et al., 2009). In contrast, the use of tetramers permits easy and rapid detection including the phenotypic characterization of antigen-sensitized cells at a single cell level by FC (Altman et al., 1996; Massilamany et al., 2010).

Unlike class I tetramers, the creation of class II tetramers is technically challenging and it requires stable expression of soluble monomers composed of MHC II-α and β chains. Class II tetramers were originally created by tethering peptide sequences covalently to the N-terminus of the class II-β chain, but this approach requires generation of tetramers for each peptide individually (Kozono et al., 1994; Altman et al., 1996). The newer approach involves expression of empty class II molecules into which peptides are loaded exogenously, thereby facilitating creation of tetramers utilizing a single recombinant virus (Novak et al., 2001a; Kwok et al., 2002, Day et al., 2003; Jang et al., 2003). Some empty class II molecules (*e.g.*, DQ8) tend to aggregate, requiring protection of the peptide-binding site (Jang et al., 2003), but the derivation of tetramers from CLIP precursors overcomes this disadvantage. Additionally, exogenous loading allows peptides to bind MHC molecules in different registries (Novak et al., 2001a; Day et al., 2003; Jang et al., 2003). We adopted both peptide- and CLIP-tethered approaches to generate IA^k tetramers, validating the reagents with Myhc-α-reactive cells obtained from mice immunized with Myhc-α 334–352 using RNase 43–56 tetramers as controls.

First, we validated IA^k tetramers derived from peptide precursors. By using two tetramers (Myhc and RNase) and two cell

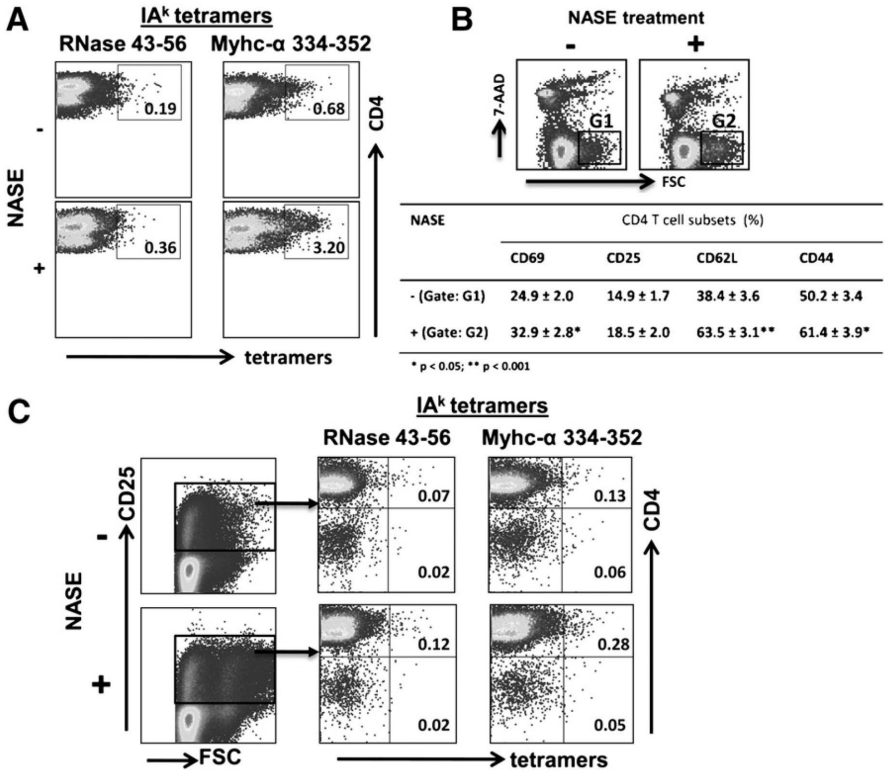

Figure 8. Enumeration of the frequency of Myhc-α 334–352-specific CD4 cells *ex vivo*. A, effect of NASE on tetramer binding. LNC from immunized mice were restimulated with Myhc-α 334–352 for 2 days followed by resting in IL-2 medium for 2 weeks. Cells were treated with or without NASE, followed by staining with tetramers, anti-CD4 and 7-AAD. After acquiring the cells by FC, tet^+ cells were enumerated in the live ($7\text{-}AAD^-$) CD4 subset. Data represents one of the three individual experiments. B, effect of NASE on T cells. A/J mice were immunized twice with Myhc-α 334–352 in CFA with an interval of 1 week. After 7 days, mice were killed and LN were harvested, and single cell suspensions were prepared. LNC were treated with or without NASE, stained with indicated markers, anti-CD4 and 7-AAD and acquired by FC. Percentages of each marker were analyzed in CD4 subset gated on 'G1 and G2' (n = 3). C, tetramer analysis *ex vivo*. LNC were obtained from mice immunized with Myhc-α 334–352 and CD4 cells were isolated by magnetic separation. After treating the cells with or without NASE, cells were stained with tetramers, anti-CD4, anti-CD25 and 7-AAD, and percentages of tet^+ cells were analyzed in the live ($7\text{-}AAD^-$) CD25-expressing CD4 subset by FC. Data representing 3 individual experiments involving 3 to 5 mice in each are shown.

types that react specifically to Myhc-α 334–352 or RNase 43–56, we demonstrated that IA^k tetramers bind to antigen-sensitized cells with specificity. The conditions optimized for tetramer staining include concentration (30 μg/ml), duration (3 h), temperature (RT), pH (7.6) and the amount of FCS in the staining medium (2.5%). We and others had previously reported similar conditions for IA^s, IA^{g7}, IA^u and IA^b tetramers, suggesting that the tetramer reaction conditions for various IA alleles are generally similar (Liu et al., 2000; Radu et al., 2000; Reddy et al., 2003; Korn et al., 2007). We noted that the staining intensity increased proportionally with the increased concentration of tetramers, but the concentration of 30 μg/ml was chosen to conserve the reagent. Likewise, the specificity of Myhc-α 334–352 tetramers was not affected by the presence or absence of FCS in the staining medium, but this component was included to keep the cells healthy in the staining reactions. Second, to enhance versatility, we sought to create tetramers utilizing IA^k/CLIP precursors, which permitted generation of Myhc-α 334–352 or RNase 43–56 tetramers by loading the peptides into CLIP-cleaved empty IA^k monomers. As previously shown (Harding et al., 1991; Sette et al., 1992), we found that a pH range of 6.0 to 7.5 facilitated peptide loading into IA^k molecules. Myhc-α tetramers derived from these IA^k/peptide complexes stained Myhc-α-reactive cells with specificity, proving that the CLIP precursors can be used to create tetramers easily, thus broadening the applications of IA^k tetramers. However, it is to be noted that the staining intensity obtained with the tetramers derived from CLIP precursors was generally less than that observed with

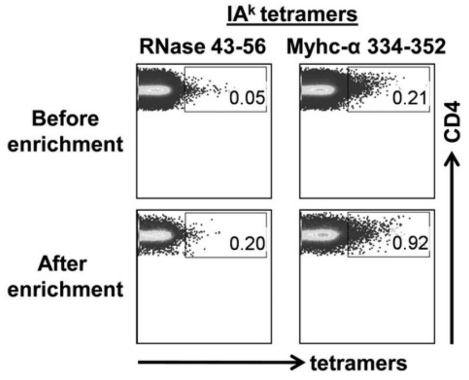

Figure 9. Enrichment of tet^+ cells *ex vivo* by magnetic separation. CD4 cells were enriched from mice immunized with Myhc-α 334–352 on day 14 postimmunization by negative selection based on magnetic separation. Cells were then treated with NASE followed by staining with PE-conjugated IA^k tetramers and anti-PE magnetic particles. After enrichment, cells were washed and stained with anti-CD4 and 7-AAD and acquired by FC and the anti-PE-bound tet^+ cells were then analyzed. Representative data from two individual experiments involving a pool of 3 to 5 mice in each are shown.

peptide-tethered tetramers. This may be due to the possibility that some of the IA^k molecules in tetramers made from CLIP precursors might not have been loaded with the peptides as opposed to peptide-tethered tetramers in which every IA^k molecule is embedded with a peptide.

In our previous experience with IA^s tetramers, which were created to detect PLP 139–151-specific CD4 cells in SJL mice, we had noted that tetramer binding peaked between days 4 and 6 poststimulation with PLP 139–151, but the staining became negligible by day 10 (Reddy et al., 2003). In contrast, convincing evidence of staining occurred with Myhc-α tetramers in LNC stimulated with Myhc-α 334–352 for at least 4 days after preparation. The staining increased progressively but persisted even up to day 10. This observation is critical to note because we generally use antigen-stimulated cells within 4 days after activation for adoptive transfer experiments, and our data indicated that antigen-specific T cell expansion occurs rather slowly in A/J mice. Whether such a slow expansion is a characteristic of particular immunogens or mouse strains remains to be determined. Importantly, under similar conditions, we failed to obtain Myhc-α 334–352-responsive T cell cultures from splenocytes harvested from immunized mice. Although it is expected that antigen-sensitized T cells are more concentrated in draining LN than in spleens, the lack of T cell responses in the latter implies that the use of splenocytes is not a viable option to determine antigen-specific T cell reactivity, at least for Myhc-α 334–352. Our data suggest that the antigen-stimulated LNC but not splenocyte cultures maintained in IL-2 medium for approximately 8–10 days are better suited for functional studies in A/J mice.

We and others had previously shown that class II tetramers have a greater tendency to bind activated cells (Cameron et al., 2001; Novak et al., 2001b; Reddy et al., 2003; Reijonen et al., 2003). Contrary to our expectations, we noted that Myhc-α tetramers showed a preference for rested or unactivated cells expressing low levels of CD25. Conceivably, because tetramer binding requires high-affinity T cell receptor (TCR) interactions, cells bearing low-affinity TCRs may fail to be detected by tetramers (Mallet-Designe et al., 2003; Reddy et al., 2003; Vollers and Stern, 2008). The lack of significant binding to the $CD25^{high}$ subset suggests that the affinity of TCRs of Myhc-α-reactive cells may differ between $CD25^{low}tet^+$ and $CD25^{high}tet^+$ populations. Alternatively, the differential binding of tetramers to $CD25^{low}$ and $CD25^{high}$ subsets might be due to differences in TCR clustering/densities or their organization in the respective populations. For example, TCR clustering was inversely correlated with CD25 expression in the transgenic T cells bearing high-affinity TCRs specific to myelin basic proteins 1–9 (Pastor et al., 2006). Likewise, in the CD8 T cell system involving hemagglutinin 533–541-specific TCRs, transient loss of tetramer binding was noted in relation to increased expression of CD25 shortly after antigen stimulation, and this phenomenon was ascribed to change in the display or organization of TCRs (Drake et al., 2005). Previously, it was shown that CD40L expression can be used as a marker of antigen-specific cells (Chattopadhyay et al., 2005; Frentsch et al., 2005); we therefore expected that binding of Myhc-α tetramers would correlate with CD40L expression, but this was not the case. This discrepancy could be due to the fact that we performed tetramer analysis in relation to CD40L-expression on day 8 poststimulation with Myhc-α 334–352, the time point at which tetramer staining intensity reached its peak (Figure 5A), as opposed to 6 h at which CD40L expression was examined previously (Frentsch et al., 2005). It should be noted that Myhc-α tetramers cannot be used to stain cells immediately after antigen stimulation for at least 4 days because of their inability to bind antigen-reactive cells with specificity. Therefore, lack of correlation between tetramer binding and CD40L expression does not mean that CD40L-expressing cells are not antigen-specific. Alternatively, the class II tetramers may be inherently limited in binding only to high-affinity TCR-bearing cells, and the appearance of tet^+CD40L^+ and tet^+CD40L^- subsets may represent antigen-reactive cells containing high- and low-affinity TCRs, respectively.

One objective of deriving tetramers is the ability to enumerate the frequency of antigen-specific cells *ex vivo*, obviating the need to stimulate the cells *in vitro*. Accumulated literature suggests that class II tetramers bind activated cells, but not resting cells, even though they are antigen-specific (Cameron et al., 2001; Novak et al., 2001b; Reddy et al., 2003; Reijonen et al., 2003). This makes it difficult to accurately determine the frequencies of antigen-specific T cell repertoires. To overcome this limitation, we adopted a strategy of exposing the cells to NASE prior to tetramer staining (Daniels et al., 2001; Reddy et al., 2003), which facilitated detection of approximately two-fold more with Myhc-α tet^+ cells than those detected without NASE in mice immunized with Myhc-α 334–352. The enhanced binding of Myhc-α tetramers obtained with NASE treatment may be due to two mechanisms: 1) NASE may enhance adhesiveness between TCR and tetramers by removing sialic acid from the cell surface, thereby reducing the net charge (Krieger et al., 1988; Daniels et al., 2001), or 2) NASE can nonspecifically activate T cells (Krieger et al., 1988; Reddy et al., 2003). Since activated cells generally can be bound better by class II tetramers, we activated LNC obtained from immunized mice transiently for 6–12 h with various polyclonal activators (such as CD3, TCR and CD28 antibodies, phorbol 12-myristate 13-acetate/ionomycin, and superantigens), but none of these agents enhanced either the sensitivity or specificity of Myhc-α-reactive cells (data not shown). Although low, background staining with RNase tetramers was consistently noted in *ex vivo* staining reactions. We chose the bovine sequence for RNase 43–56 as a control, and the bovine sequence is 92% similar to mouse RNase, except that serine at position 50 in bovine RNase is substituted with proline in the mouse. It has been shown that the naïve peripheral repertoires contain autoreactive T cells for various self-antigens (Klein and Kyewski, 2000; Romagnani, 2006; Root-Bernstein, 2007). Whether RNase tet^+ cells represent such a pool is not known, and we did not pursue this aspect in our studies.

In summary, we have demonstrated that IA^k/Myhc-α tetramers facilitate the detection of Myhc-α 334–352-reactive CD4 cells with specificity. The tetramers are helpful tools to characterize the appearance, disappearance and persistence of cardiac myosin-reactive CD4 T cell repertoires in mice bearing the H-2/IA^k allele. These include A/J, B10.A, B10.BR and CBA/J mice, which show varying degrees of autoimmune responses to cardiac myosin (Neu et al., 1987b; Smith and Allen, 1991; Donermeyer et al., 1995). For example, A/J, CBA/J and B10.BR mice are highly susceptible to EAM and Coxsackievirus B3-induced myocarditis, whereas B10.A mice are relatively resistant

(Wolfgram et al., 1986; Neu et al., 1987a; Neu et al., 1987b; Leslie et al., 1990; Gauntt et al., 1995). Our data obtained with the EAM protocol suggest that myosin-specific CD4 cells can be reliably enumerated in LNC but not in splenocytes, and that NASE treatment prior to tetramer staining facilitates detection of antigen-specific cells *ex vivo*. From the practical stand point, IA^k tetramers could serve as useful tools to enumerate the precursor frequencies of antigen-specific cells in cultures expanded *in vitro* since activation facilitates efficient binding of IA^k tetramers. Because of this limitation, it is difficult to accurately analyze the frequencies of Myhc-α 334–352-specific cells *ex vivo*.

Acknowledgments — We thank Hongjiu Dai for his involvement in the partial creation of IA^k constructs.

References

Altman, J.D., Moss, P.A., Goulder, P.J., Barouch, D.H., McHeyzer-Williams, M.G., Bell, J.I., McMichael, A.J., Davis, M.M., 1996. Phenotypic analysis of antigen-specific T lymphocytes. Science 274, 94.

Baker, R.L., Wagner Jr., D.H., Haskins, K., 2008. CD40 on NOD CD4 T cells contributes to their activation and pathogenicity. J. Autoimmun. 31, 385.

Buckner, J.H., Holzer, U., Novak, E.J., Reijonen, H., Kwok, W.W., Nepom, G.T., 2002. Defining antigen-specific responses with human MHC class II tetramers. J. Allergy Clin. Immunol. 110, 199.

Cameron, T.O., Cochran, J.R., Yassine-Diab, B., Sekaly, R.P., Stern, L.J., 2001. Cutting edge: detection of antigen-specific CD4+ T cells by HLA-DR1 oligomers is dependent on the T cell activation state. J. Immunol. 166, 741.

Carneiro, J., Duarte, L., Padovan, E., 2009. Limiting dilution analysis of antigen-specific T cells. Methods Mol. Biol. 514, 95.

Chattopadhyay, P.K., Yu, J., Roederer, M., 2005. A live-cell assay to detect antigen-specific CD4+ T cells with diverse cytokine profiles. Nat. Med. 11, 1113.

Daniels, M.A., Devine, L., Miller, J.D., Moser, J.M., Lukacher, A.E., Altman, J.D., Kavathas, P., Hogquist, K.A., Jameson, S.C., 2001. CD8 binding to MHC class I molecules is influenced by T cell maturation and glycosylation. Immunity 15, 1051.

Day, C.L., Seth, N.P., Lucas, M., Appel, H., Gauthier, L., Lauer, G.M., Robbins, G.K., Szczepiorkowski, Z.M., Casson, D.R., Chung, R.T., Bell, S., Harcourt, G., Walker, B.D., Klenerman, P., Wucherpfennig, K.W., 2003. Ex vivo analysis of human memory CD4 T cells specific for hepatitis C virus using MHC class II tetramers. J. Clin. Invest. 112, 831.

Donermeyer, D.L., Beisel, K.W., Allen, P.M., Smith, S.C., 1995. Myocarditis inducing epitope of myosin binds constitutively and stably to I-Ak on antigen-presenting cells in the heart. J. Exp. Med. 182, 1291.

Drake III, D.R., Ream, R.M., Lawrence, C.W., Braciale, T.J., 2005. Transient loss of MHC class I tetramer binding after CD8+ T cell activation reflects altered T cell effector function. J. Immunol. 175, 1507.

Frentsch, M., Arbach, O., Kirchhoff, D., Moewes, B., Worm, M., Rothe, M., Scheffold, A., Thiel, A., 2005. Direct access to CD4+ T cells specific for defined antigens according to CD154 expression. Nat. Med. 11, 1118.

Gauntt, C.J., Tracy, S.M., Chapman, N., Wood, H.J., Kolbeck, P.C., Karaganis, A.G., Winfrey, C.L., Cunningham, M.W., 1995. Coxsackievirus-induced chronic myocarditis in murine models. Eur. Heart J. 16 (Suppl. O), 56.

Harding, C.V., Roof, R.W., Allen, P.M., Unanue, E.R., 1991. Effects of pH and polysaccharides on peptide binding to class II major histocompatibility complex molecules. Proc. Natl. Acad. Sci. U. S. A. 88, 2740.

Hill, S.L., Afanasyeva, M., Rose, N.R., 2002. Autoimmune myocarditis. In: Theofilopoulos, A.N., Bona, C.A. (Eds.), The Molecular Pathology of Autoimmune Diseases. Taylor & Francis Inc., New York, p. 951.

Jang, M.H., Seth, N.P., Wucherpfennig, K.W., 2003. Ex vivo analysis of thymic CD4 T cells in nonobese diabetic mice with tetramers generated from I-A(g7)/class II-associated invariant chain peptide precursors. J. Immunol. 171, 4175.

Klein, L., Kyewski, B., 2000. "Promiscuous" expression of tissue antigens in the thymus: a key to T-cell tolerance and autoimmunity? J. Mol. Med. 78, 483.

Kodama, M., Matsumoto, Y., Fujiwara, M., Masani, F., Izumi, T., Shibata, A., 1990. A novel experimental model of giant cell myocarditis induced in rats by immunization with cardiac myosin fraction. Clin. Immunol. Immunopathol. 57, 250.

Korn, T., Reddy, J., Gao, W., Bettelli, E., Awasthi, A., Petersen, T.R., Backstrom, B.T., Sobel, R.A., Wucherpfennig, K.W., Strom, T.B., Oukka, M., Kuchroo, V.K., 2007. Myelin-specific regulatory T cells accumulate in the CNS but fail to control autoimmune inflammation. Nat. Med. 13, 423.

Kozono, H., White, J., Clements, J., Marrack, P., Kappler, J., 1994. Production of soluble MHC class II proteins with covalently bound single peptides. Nature 369, 151.

Krieger, J., Jenis, D.M., Chesnut, R.W., Grey, H.M., 1988. Studies on the capacity of intact cells and purified Ia from different B cell sources to function in antigen presentation to T cells. J. Immunol. 140, 388.

Kwok, W.W., Ptacek, N.A., Liu, A.W., Buckner, J.H., 2002. Use of class II tetramers for identification of CD4+ T cells. J. Immunol. Methods 268, 71.

Leslie, K.O., Schwarz, J., Simpson, K., Huber, S.A., 1990. Progressive interstitial collagen deposition in Coxsackievirus B3-induced murine myocarditis. Am. J. Pathol. 136, 683.

Liao, L., Sindhwani, R., Leinwand, L., Diamond, B., Factor, S., 1993. Cardiac alpha-myosin heavy chains differ in their induction of myocarditis. Identification of pathogenic epitopes. J. Clin. Invest. 92, 2877.

Liu, C.P., Jiang, K., Wu, C.H., Lee, W.H., Lin, W.J., 2000. Detection of glutamic acid decarboxylase-activated T cells with I-Ag7 tetramers. Proc. Natl. Acad. Sci. U. S. A. 97, 14596.

Mallet-Designe, V.I., Stratmann, T., Homann, D., Carbone, F., Oldstone, M.B., Teyton, L., 2003. Detection of low-avidity CD4+ T cells using recombinant artificial APC: following the antiovalbumin immune response. J. Immunol. 170, 123.

Mallone, R., Nepom, G.T., 2004. MHC class II tetramers and the pursuit of antigen-specific T cells: define, deviate, delete. Clin. Immunol. 110, 232.

Massilamany, C., Steffen, D., Reddy, J., 2010. An epitope from Acanthamoeba castellanii that cross-react with proteolipid protein 139–151-reactive T cells induces autoimmune encephalomyelitis in SJL mice. J. Neuroimmunol. 219, 17.

Neu, N., Beisel, K.W., Traystman, M.D., Rose, N.R., Craig, S.W., 1987a. Autoantibodies specific for the cardiac myosin isoform are found in mice susceptible to Coxsackievirus B3-induced myocarditis. J. Immunol. 138, 2488.

Neu, N., Rose, N.R., Beisel, K.W., Herskowitz, A., Gurri-Glass, G., Craig, S.W., 1987b. Cardiac myosin induces myocarditis in genetically predisposed mice. J. Immunol. 139, 3630.

Novak, E.J., Liu, A.W., Gebe, J.A., Falk, B.A., Nepom, G.T., Koelle, D.M., Kwok, W.W., 2001a. Tetramer-guided epitope mapping: rapid identification and characterization of immunodominant CD4+ T cell epitopes from complex antigens. J. Immunol. 166, 6665.

Novak, E.J., Masewicz, S.A., Liu, A.W., Lernmark, A., Kwok, W.W., Nepom, G.T., 2001b. Activated human epitope-specific T cells identified by class II tetramers reside within a CD4high, proliferating subset. Int. Immunol. 13, 799.

Otani, T., Tsuji-Takayama, K., Okochi, A., Yamamoto, M., Takeuchi, M., Yamasaki, F., Nakamura, S., Kibata, M., 2011. Stromal cells' B7-1 is a key stimulatory molecule for interleukin-10 production by HOZOT, a multifunctional regulatory T-cell line. Immunol. Cell Biol. 89, 246.

Pastor, S., Vaccaro, C.G., Minguela, A., Ober, R.J., Ward, E.S., 2006. Analyses of TCR clustering at the T cell-antigen-presenting cell interface and its impact on the activation of naive CD4+ T cells. Int. Immunol. 18, 1615.

Pummerer, C.L., Luze, K., Grassl, G., Bachmaier, K., Offner, F., Burrell, S.K., Lenz, D.M., Zamborelli, T.J., Penninger, J.M., Neu, N., 1996. Identification of cardiac myosin peptides capable of inducing autoimmune myocarditis in BALB/c mice. J. Clin. Invest. 97, 2057.

Radu, C.G., Anderton, S.M., Firan, M., Wraith, D.C., Ward, E.S., 2000. Detection of autoreactive T cells in H-2u mice using peptide-MHC multimers. Int. Immunol. 12, 1553.

Reddy, J., Bettelli, E., Nicholson, L., Waldner, H., Jang, M.H., Wucherpfennig, K.W., Kuchroo, V.K., 2003. Detection of autoreactive myelin proteolipid protein 139–151-specific T cells by using MHC II (IAs) tetramers. J. Immunol. 170, 870.

Reijonen, H., Kwok, W.W., Nepom, G.T., 2003. Detection of CD4+ autoreactive T cells in T1D using HLA class II tetramers. Ann. N. Y. Acad. Sci. 1005, 82.

Reiser, P.J., Portman, M.A., Ning, X.H., Schomisch Moravec, C., 2001. Human cardiac myosin heavy chain isoforms in fetal and failing adult atria and ventricles. Am. J. Physiol. Heart Circ. Physiol. 280, H1814.

Romagnani, S., 2006. Immunological tolerance and autoimmunity. Intern. Emerg. Med. 1, 187.

Root-Bernstein, R., 2007. Antigenic complementarity in the induction of autoimmunity: a general theory and review. Autoimmun. Rev. 6, 272.

Sette, A., Southwood, S., O'Sullivan, D., Gaeta, F.C., Sidney, J., Grey, H.M., 1992. Effect of pH on MHC class II-peptide interactions. J. Immunol. 148, 844.

Smith, S.C., Allen, P.M., 1991. Myosin-induced acute myocarditis is a T cellmediated disease. J. Immunol. 147, 2141.

Vollers, S.S., Stern, L.J., 2008. Class II major histocompatibility complex tetramer staining: progress, problems, and prospects. Immunology 123, 305.

Wolfgram, L.J., Beisel, K.W., Herskowitz, A., Rose, N.R., 1986. Variations in the susceptibility to Coxsackievirus B3-induced myocarditis among different strains of mice. J. Immunol. 136, 1846.

Zhang, P., Sun, D., Ke, Y., Kaplan, H.J., Shao, H., 2007. The net effect of costimulatory blockers is dependent on the subset and activation status of the autoreactive T cells. J. Immunol. 178, 474.